

CROSSSHORE SAND PATTERNS IN THE INTERTIDAL ZONE: A CASE STUDY WITH PERMANENT LASER SCANNING AT KIJKDUIN BEACH

S.E. VOS¹, R.N.P. HOBBELEN², L. SPAANS¹, S. DE VRIES¹
AND R.C. LINDENBERGH³

1. *Delft University of Technology, Department of Hydraulic Engineering, Stevinweg 1, 2628 CN Delft, S.E.Vos@tudelft.nl, L.Spaans@student.tudelft.nl and Sierd.deVries@tudelft.nl.*
2. *Waterboard Brabantse Delta, Bouvignelaan 5, 4836 AA Breda, r.hobbelen@brabantsedelta.nl*
3. *Delft University of Technology, Department of Geoscience and Remote Sensing, Stevinweg 1, 2628 CN Delft, r.c.lindenbergh@tudelft.nl.*

Abstract: The intertidal zone is an important coastal zone linking the shore with the sea and it acts as an interface between the marine and aeolian zone facilitating the transfer of sand underwater and the beach. It is an extreme environment where water, sediment, wind and ecology constantly interact with each other under continuously changing conditions which impede the acquirement of reliable measurements. The utilization of a permanent laser scanner within the CoastScan project has provided the opportunity to monitor the beach hourly for a six month period resulting in a detailed image of the height variations of the intertidal zone. The analysis of the data shows the development of multiple bars in the intertidal area which can partly be coupled to external meteorological and hydrodynamic conditions.

Introduction

The intertidal zone is an important coastal boundary found worldwide linking the shore and the sea. The zone extends from the lowest to the highest observed water level of the local tide with vertical ranges up to 17 meters. It is an important ecological zone and has a significant influence on the shape of the coast.

On sandy coasts the intertidal zone is an important interface between the marine and aeolian zones of the sediment sharing coastal system. It facilitates the transfer of sand from below water to the beach during mild conditions and back under water during storm conditions and is therefore the backbone of the development of the coastline. It is an extreme environment where water, sediment, wind and ecology constantly interact with each other under continuously changing conditions. Recent research (Luijendijk et al,2018) has indicated that about 80000 km of the sandy coasts worldwide encounter

retreating coastlines. Although parts of the retreats can be linked to human intervention about 40% of the retreats cannot easily be explained. With increasing sea surface level rise due to the climate change and an increasing number of people living close to the sea it is important to understand the processes in the intertidal zone and their influences on the coastal evolution.

Part of the problem is that not all processes in the intertidal zone are completely understood and cannot completely be reproduced. The erosive processes can reasonably well be modeled with models like XBeach (Roelvink et al, 2009) but restorative processes are harder to reproduce. While these uncertainties exist several hypothesis are posed on the role of the intertidal zone in the exchange of sediment between marine and aeolian zones. Houser et al., (2009) hypothesizes that the synchronization of physical processes associated with sediment transport and supply between the zones are the main force for the sediment exchange between zones. Along these lines, Cohn et al., (2017) have focused on the process of bar welding and initiated a model that includes both marine and aeolian processes to describe the sediment exchange.

The impact of these efforts are however somewhat limited because data on the specific processes in the intertidal area are very scarce. Part of the problem is obtaining reliable information in the zone with a challenging and ever changing environment. Constant wetting and drying with high concentration sediment flows, currents and waves make the environment hard for measurements. Often an array of instruments is used (Raubenheimer et al, 2018) to collect suitable information. These range from pressure sensors, ADCP's to jet ski hydrography, lidar and GPS measurements. Often these measurements are labor intensive or need stationary frames (or anchor points) which are susceptible to constant wetting and drying, burrowing and to human interference during low tides.

Permanent laser scanning of the beach, (CoastScan, Vos et. al., 2017, O'Dea et al 2016, Raubenheimer et al, 2018) provides a relative new alternative method to obtain undisturbed high quality measurements in the intertidal zone. These measurements allow for studying the region for extended periods of time without the environmental or human interference and the associated costs. Previously (Lindenbergh et al., 2011, Bitenc et al., 2011), it was shown that repetitive beach scanning is able to reveal changes at the cm to mm scale, but permanent setups only recently became available. These setups differ from the more usual use of (air or car based) mobile laser (Sallenger et al., 2003, Donker et al., 2018) which often inhibit a lower sampling rate but a larger survey area.

This paper will present the first analysis of a 6 month field data set of measured intertidal morphology obtained using hourly laser scans during an extensive field campaign at Kijkduin (The Netherlands) from November 2016 to May 2017.

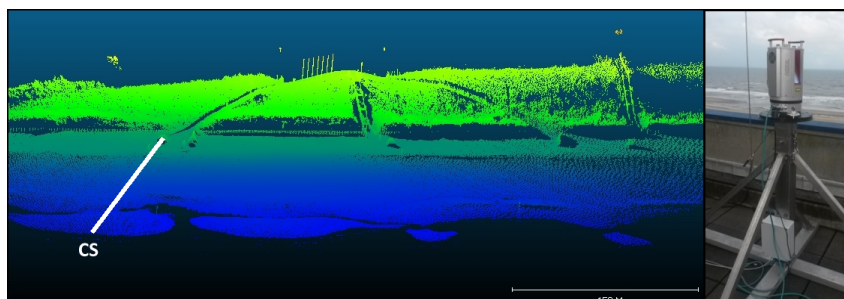


Figure 1. Example of a laser scan showing the beach and dune area at Kijkduin (left) obtained with the Riegl laser scanner VZ 2000 (right). The white line (left) indicates the cross-section (CS) analyzed in this article.

Data

Field experiment

The field campaign was conducted at Kijkduin (The Netherlands). The field site is located north of the Sand Motor (Stive et al, 2013) and was selected due the availability of an excellent observation point on top of Hotel Atlantic situated next to the dunes and the sea. Data was available from 11th November 2016 to 26th may 2017, but due to data gaps analysis was performed from 1st January to 26th may 2017. Data consisted of hourly $0.05^{\circ} \times 0.05^{\circ}$ degree scans of the morphology of the beach and dunes (see figure 1) obtained with a Riegl VZ 2000 laser scanner. Each scan of the beach contains about 800000 points with an average horizontal resolution of 50 centimeters along the waterline. For analysis one low water scan was selected per day. Due to mist and other weather influences a total of four days with low quality scans were skipped. The data is georeferenced with a total of 5 reflectors around the laser scanner (see Vos et. al., 2017 for more details).

Data processing

All data is processed with the procedure schematized in figure 2. The focus was on obtaining cross-sections of the beach usable for analysis (See figure 1 for the location). For computational reasons each scan was cropped in the first step to obtain a smaller patch of sand through which a cross section could be obtained. The patch runs from the top of the berm to the waterline.

After cropping the data was cleaned from e.g. outliers with the lasnoise function of the LasTools software (LAsTools, 2014). The software removes points that have too few neighboring points. A box (step) size of 2 meters and isolated point count threshold of 8 was used. On average less than 0.1% of the points were removed after noise filtering mostly consisting of water/wave reflection points. As a comparison data was also cleaned by hand and on average lasnoise

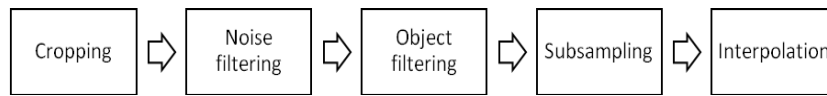


Figure 2: Data processing procedure.

only missed $2.61 \cdot 10^{-4}\%$ of the points removed by hand. As a final step the data was subsampled and interpolated to obtain consisting cross-sections.

Data quality

An initial data quality analysis was performed in Vos et al, 2017. A more detailed analysis has shown that the laser scanner inhibits a temperature dependent variation (Anders et al, 2019). This variation is especially visible in the z-direction in the cross-sections (see figure 3A). Variations in the z-direction are in the order of 5-10 centimeter.

As an initial measure the z-variations are reduced by forcing the z-level of the upper beach (defined as the shore between 1.5 and 3 meter (m) height) to one specific level for all cross-sections (see figure 3B). The upper beach was chosen because the envelope of the observed data (see figure 3C) showed that the variation is minimal in that area. A disadvantage of the used method is that small variations in the upper beach cannot be observed. As the focus in this article is on the intertidal zone (between 0-1.5 meter height) and with a larger found variance in the intertidal zone than the upper beach this is deemed acceptable. A more advanced correction technique which omits the upper beach is currently in development.

Figure 4 shows a time stack of the laser scan data showing the behavior of the cross-section through time. The figure shows that the length of the cross-section can vary from day to day. Linear regression with tidal range, precipitation, radiation, relative humidity and time of day shows no significant relation between the cross-section length and these parameters. Maybe it is connected to surface moisture or the ground water level but up to now the variation in length cannot be explained and correlated to an external climatological or hydrodynamic parameter.

The data quality in the lowest reaches of the cross-sections deprecates significantly in the direction of the waterline. This can be seen in figure 3C where the mean profile becomes more jagged and shows more straight lines (due to interpolation) towards the sea. A possible reason could be the increased water concentration in the sand as the laser scanner experiences problems with wet areas although more research is needed to confirm this completely. The area will therefore not be included in the analysis shown in this paper.

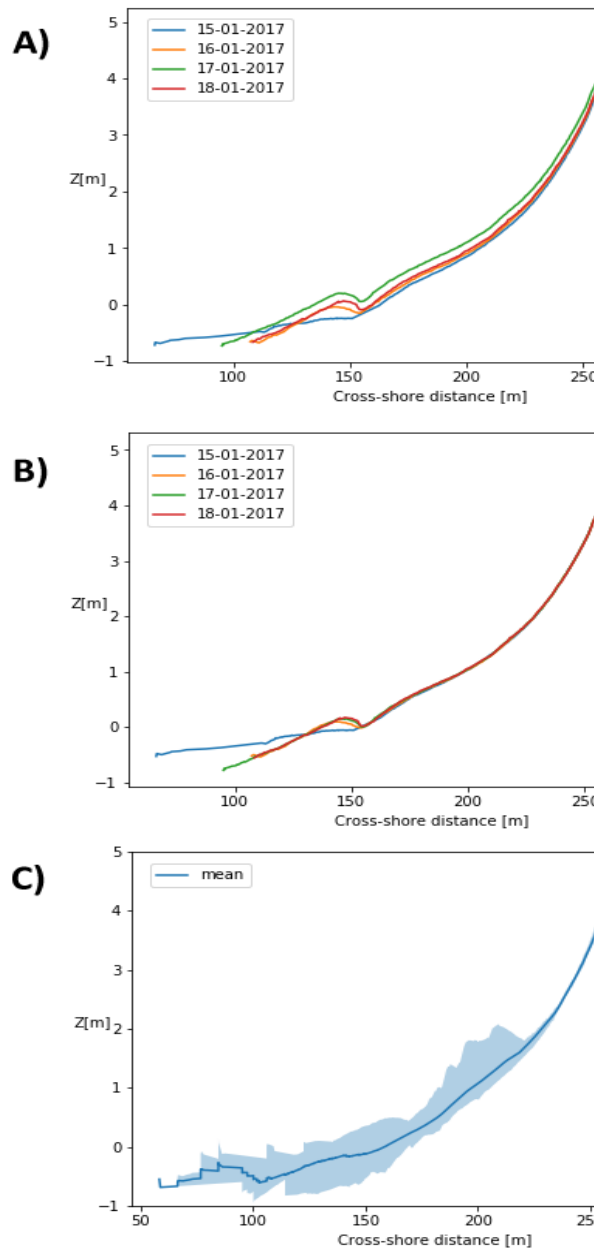


Figure 3. Observed (A) and corrected (B) data variance for several days in January 2017 and observed mean profile and envelop (c)

for the whole data series.

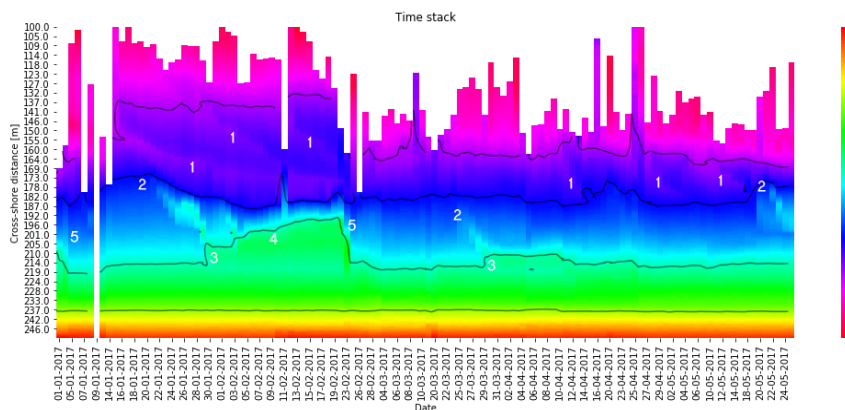


Figure 4: Time stack of all cross-sections (height in m. N.A.P.). The colour scale represents elevation and contour lines are indicated in black, at NAP +0 m., NAP+0.5 m., NAP+1.5 m., NAP+2.5. Numbers indicate different features on the beach; 1) Low amplitude incoming bar which are flooded during high tide; 2) High amplitude bar formed during upcoming tide along the water line; 3): Bar attachment to the beach during spring tide; 4): Bar expands in offshore direction and 5): Bar eroded due to storm.

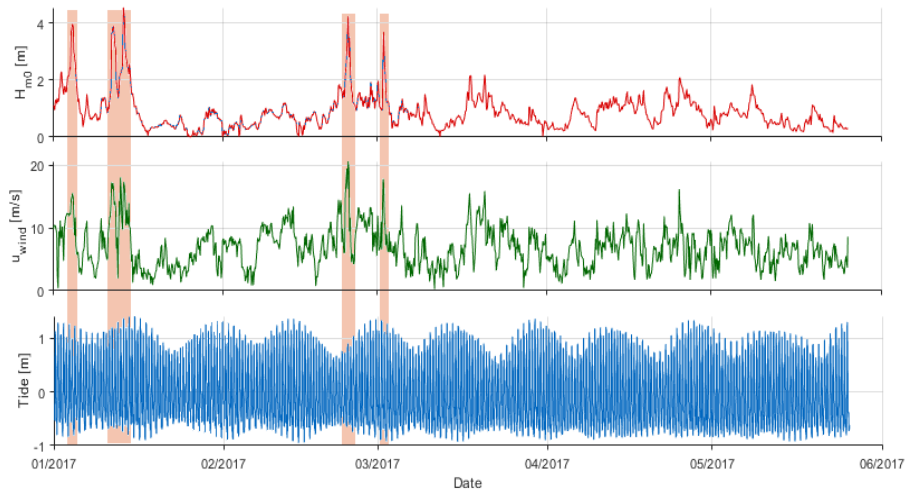


Figure 5: Wave (top graph), wind speed (middle graph) and tide (bottom graph) during the measurement period. Red areas indicate show storm periods.

Results

The cross-sections in figure 4 show various sand bars. Six low amplitude bars migrate shoreward in the swash zone (visible between the 0-0.5 meter height contours; indicated by 1 in figure 4) while 4 larger bars migrate shoreward around the high waterline (0.5-1.5 meter height contours; 2 in figure 4). With an average height of 20 cm the bars in the swash zone are about a third of the bars of 60 cm observed around the high water line. The smaller bars turn away to the 0.5 meter height contour and don't connect with the larger sandbars. The larger bars around the high waterline move shoreward with the upcoming tide. This is especially clear for the bar which originated around 20th January 2017 at the high waterline. It moves shoreward and it welds and extends thereafter to the beach (3-4, figure 4) with the neap-spring tidal cycle.

Figure 6 clearly shows the shoreward migration of this bar in relation to the tidal range. With increasing tidal range, the bar moves onshore while its approximate location stays the same with decreasing range. With the decreasing range the bar is enlarged at the seaward side hereby widening the bar. The offshore movement in the graph around 190 meters is caused by the steepening of the bar and not so much due to a shoreward movement of the swash bar. During the migration, the peak of the bar is always located above the maximum high water level, indicating the migration occurs as a result of swash motion. Besides the increasing tidal range, wave and wind conditions are moderate between 20-1-2017 to 2-2-2017 during the migration of the bar (see image 5).

Several storms occurred during the measuring period (see figure 5). The storms eradicate the bars and flatten the beach (5, figure 4). Due to the storms it is not possible to see if the smaller bars merge with the larger sandbars around the high water line.

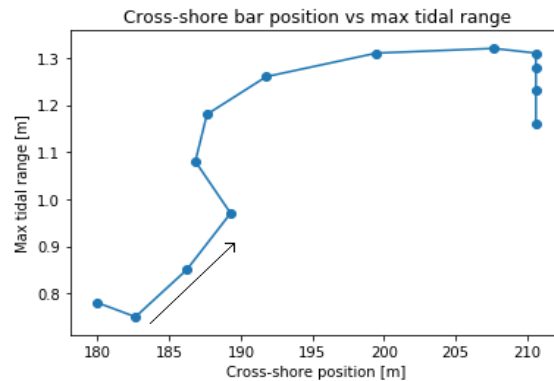


Figure 6: Cross-shore position bar vs tidal range. The arrow shows the time from 20-1-2017 to 2-2-2017.

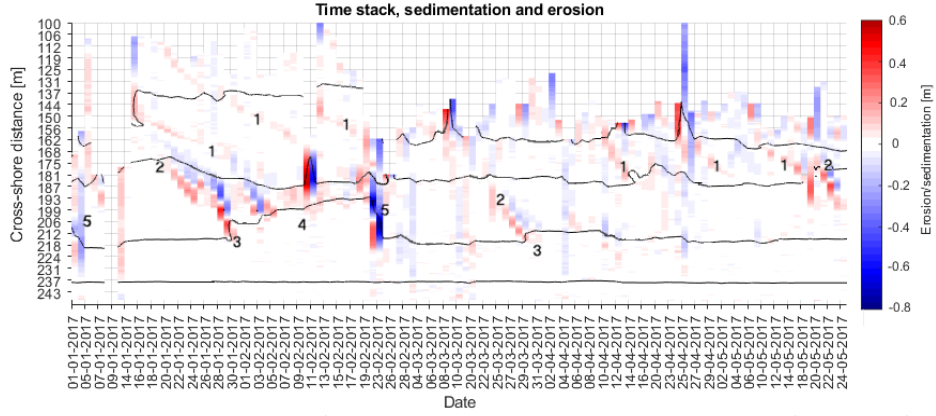


Figure 7: Sedimentation and erosion flux based on daily cross-section measurements. For reference with figure 4 contour lines are indicated in black, at NAP +0 m., NAP+0.5 m., NAP+1.5 m., NAP+2.5 and number 1-5 indicating different features on the beach.

The daily cross-sections provide the possibility to calculate cross-shore sand transport rates. Figure 7 shows the calculated height difference per 24 hours. Height changes range from -0.8 to 0.6 meter with the largest changes found around the waterline connected to the formation of the bars. The features identified in figure 4 are clearly visible. The bars in the swash zone (1, figure 7) are mostly visible as sedimentation patterns and not so much as erosion patterns. On the other and the bars around the high water (2, figure 7) line clearly show a combined sedimentation and erosion pattern during the shoreward movement. The storms (5, figure 7) clearly show concentrated erosion over almost the length of the cross section.

Based on the cross-shore time difference it is possible to estimate the cross-shore sediment transport with a simplified mass conservation function:

$$\frac{\partial z_b}{\partial t} = \frac{\partial Q}{\partial x} + \frac{\partial Q}{\partial y} \cong \frac{\partial Q}{\partial x}$$

(1)

with z_b , the bed level [m] and Q_x and Q_y the deposited volume transport in the cross-shore and along shore direction [m^2/s]. Here, for the daily transports it is assumed that the alongshore sediment transport is much smaller than the cross-shore sediment transport.

In an initial investigation (see figure 8) the sand transport volume was analyzed for five subsequent days from 26th-31st January 2017 when the bar is formed around the high water line. It clearly shows the associated erosion and sedimentation patterns at a max of about 0.5 m^2 a day with the forming of the

bar (2-3, figure 4) and the integrated sand transport Q (integrated into the waterline direction) at a max of about 5 m^3 a day.

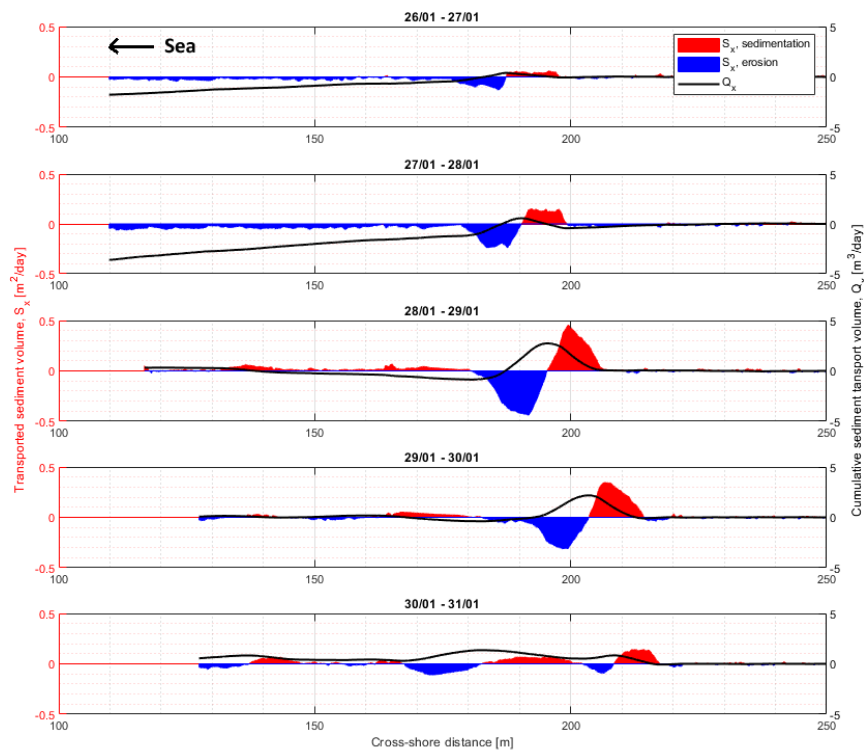


Figure 8: Transported sediment volume per meter width (m^3/m) and cumulative transport (indicated with Q) from the 26th to the 31st of January 2017.

In the first two days (26-27/01 and 27-28/01) the figure shows limited erosion over most length of the cross section and the integrated sand transport Q shows a decreasing trend towards the sea. It is at present not clear if the phenomena originate from errors in the data and/or it is an actual erosion trend during the forming of the bar.

During the shoreward migration the erosion and sediment fluxes increase in the first four days and then flatten out due to a flattening of the tidal range (see figure 6). This is also reflected in the total sand transport which peaks around 28-29/01.

Conclusion

In this article a five month period of daily low waters during 2017 has been studied with permanent laser scanning. An automated process has been designed to automatically clean the associated point clouds and to obtain accurate cross-sections. Initial results show a multitude of bar behavior in the intertidal zone during the five month period. Bars in the swash zone of about max 20cm emerge multiple times and bars of about max 60 cm originate along the waterline with upcoming tides until storms clear the bars of the beach. The daily cross sections allow for a daily sand transport analysis with erosion and sedimentation fluxes of up to 0.5 m^2 and a total sand transport up to 5 m^3 per day.

Acknowledgements

The work in this article was financed by the ERC-Advanced grant 291206-Nearshore Monitoring and Modeling (NEMO, <http://nemo.citg.tudelft.nl/>) and the CoastScan project 2018/STW/00505023. The authors wish to thank the owner and manager of the Hotel NH Atlantic Den Haag (www.nh-hotels.nl) for supporting the research by use of the hotel for the measurements. Additional thanks goes to Baars-CIPRO (www.baars-cipro.nl) for advice and the construction of the measuring frame and operational support.

References

- Anders, K., Lindenbergh, R.C., Vos, S.E., Mara, H., de Vries, S., Höfle, B. (2019), "High-frequency 3D geomorphic observation using hourly terrestrial laser scanning data of a sandy beach", *The ISPRS Geospatial Week 2019 (In press)*
- Axelsson, P., (2000), "DEM generation from Laser Scanner data using adaptive TIN Models", *International Archives of the Photogrammetry, Remote Sensing and Spatial Information Sciences*, XXXIII(Pt.B4/1):110-117
- Bitenc, M., Lindenbergh, R., Khoshelham, K., & Van Waarden, A. P. (2011). "Evaluation of a LiDAR land-based mobile mapping system for monitoring sandy coasts", *Remote Sensing*, 3(7), 1472-1491.

Cohn, N., Ruggiero, P., de Vries, S., Garcia-Medina, G. (2017), " *Beach Growth Driven by Intertidal Sandbar Welding* " ,. Proceedings of Coastal Dynamics 2017 199

O'Dea, A., Whitesides, E.T., Brodie, K. and Spore, N. (2016), " *Observations of beach cusp evolution using a stationary, shore-based lidar system* ", American Geophysical Union, Fall Meeting 2016, abstract #EP23A-0947

Donker, J., van Maarseveen, M., and Ruessink, G. (2018), " *Spatio-Temporal Variations in Foredune Dynamics Determined with Mobile Laser Scanning* ", Journal of Marine Science and Engineering 6 (4), 126

Kroon, A., & Masselink, G. (2002), " *Morphodynamics of intertidal bar morphology on a macrotidal beach under low-energy wave conditions, North Lincolnshire, England.* ", Marine geology, 190(3-4), 591-608.
LAStools, (2014), " *Efficient LiDAR Processing Software* " ,obtained from <http://rapidlasso.com/LAStools>

Lindenbergh, R. C., Soudarissanane, S. S., De Vries, S., Gorte, B. G., and De Schipper, M. A. (2011),. " *Aeolian beach sand transport monitored by terrestrial laser scanning* ", *The Photogrammetric Record*, 26(136), 384-399

Luijendijk, A. P., Ranasinghe, R., de Schipper, M. A., Huisman, B. A., Swinkels, C. M., Walstra, D. J., & Stive, M. J. (2017). The initial morphological response of the Sand Engine: A process-based modelling study. *Coastal engineering*, 119, 1-14.

Luijendijk, A. Hagenaaars, G., Ranasinghe, R. Baart, F., Donchyts., and Aarninkhof, S. (2018). " *The state of the world's beaches* ", Scientific Reports, 8(1), 6641

Raubenheimer, B., Elgar, S., Brodie, K., Spore, N., Gorrell, L. and O'Dea, A. (2018). " *Wave impact and dune erosion during hurricane Matthew* ", Coastal Engineering Proceedings 1 (36), 7

Roelvink, D., Reniers, A., Van Dongeren, A., de Vries, J.v.T., Mc Call, R. and Lescinski, J. (2009). " *Modelling storm impacts on beaches, dunes and barrier islands* ", Coastal Engineering, 56(11-12), 1133-1152

Ruessink, B. G., Pape, L., & Turner, I. L. (2009), " *Daily to interannual cross-shore sandbar migration: observations from a multiple sandbar system.* " Continental Shelf Research, 29(14), 1663-1677.

Sallenger Jr., A.H., Krabill, W.B., Swift, R.N., Brock, J., List, J., Hansen, M., Holman, R.A., Manizade, S., Sontag, J., Meredith, A., Morgan, K., Yunkel, J.K., Frederick, E.B. and Stockdon, H. (2003), "*Evaluation of airborne topographic lidar for quantifying beach changes*", *J. Coastal Res.*, 19, 125–133.

Stive, M.J.F., de Schipper, M.A., Luijendijk, A.P., Aarninkhof, S.G., van Gelder-Maas, C., van Thiel de Vries, J.S. and Ranasinghe, R., (2013), "*A new alternative to saving our beaches from sea-level rise: The Sand Motor*", *Journal of Coastal Research*, 29(5), 1001-1008

Vos, S., Lindenberg, R., de Vries, S., (2017). "*CoastScan: Continuous Monitoring of Coastal Change using Terrestrial Laser Scanning*", *Proceedings of Coastal Dynamics 2017* 233, 1518-1528